ACS APPLIED MATERIALS & INTERFACES

Research Article

www.acsami.org

Revelation of the Technological Versatility of the Eu(TTA)$_3$Phen Complex by Demonstrating Energy Harvesting, Ultraviolet Light Detection, Temperature Sensing, and Laser Applications

Praveen Kumar Shahi,[†] Akhilesh Kumar Singh,[*,‡] Sunil Kumar Singh,[§] Shyam Bahadur Rai,[†] and Bruno Ullrich[‡,∥]

[†]Department of Physics, Banaras Hindu University, Varanasi 221005, India

[‡]Instituto de Ciencias Físicas, Universidad Nacional Autónoma de México, Cuernavaca, Morelos 62210, Mexico

[§]Department of Physics, Indian Institute of Technology (Banaras Hindu University), Varanasi 221005, India

[∥]Ullrich Photonics LLC, Wayne, Ohio 43466, United States

Supporting Information

ABSTRACT: We synthesized the Eu(TTA)$_3$Phen complex and present herein a detailed study of its photophysics. The investigations encompass samples dispersed in poly(vinyl alcohol) and in ethanol in order to explore the versatile applicability of these lanthanide-based materials. Details upon the interaction between Eu, TTA, and the Phen ligands are revealed by Fourier transform infrared and UV−visible absorption, complemented by steady state and temporally resolved emission studies, which provide evidence of an efficient energy transfer from the organic ligands to the central Eu^{3+} ion. The material produces efficient emission even under sunlight exposure, a feature pointing toward suitability for luminescent solar concentrators and UV light sensing, which is demonstrated for intensities as low as 200 nW/cm^2. The paper further promotes the complex's capability to be used as luminescence-based temperature sensor demonstrated by the considerable emission intensity changes of ∼4.0% per K in the temperature range of 50−305 K and ∼7% per K in the temeperature range 305−340 K. Finally, increasing the optical excitation causes both spontaneous emission amplification and emission peak narrowing in the Eu(TTA)$_3$Phen complex dispersed in poly(vinyl alcohol) - features indicative of stimulated emission. These findings in conjunction with the fairly large stimulated emission cross-section of 4.29×10^{-20} cm^2 demonstrate that the Eu(TTA)$_3$Phen complex dispersed in poly(vinyl alcohol) could be a very promising material choice for lanthanide-polymer based laser architectures.

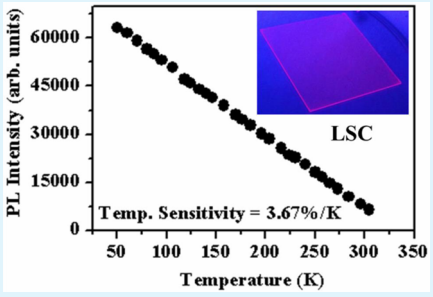

KEYWORDS: *Eu(TTA)$_3$Phen, UV light detection, temperature sensor, laser material, luminescent solar concentrators*

1. INTRODUCTION

Luminescent organic materials such as semiconducting polymers and dyes offer several appealing properties, such as, emission coverage of the entire visible spectrum, high fluorescence efficiencies, and deposition ease due to mechanical flexibility, which are very useful for photonic applications.[1,2] However, the textures of molecular conjugates are hardly able to produce monocolor-like emission spectra, while lanthanide ions emit much more narrow yet weak photoluminescence (PL) peaks. The low-intensity PL is caused by the forbidden nature of the 4f−4f transition, which caps the absorption and, as a consequence, the recombination rate.[3,4] In order to find ways to overcome the drawbacks and limitations of the organic and inorganic materials, lanthanide complexes were intensively studied as an alternative.[5−8] Notably, the heteropairing of lanthanide ions with ligands, which are composed of organic moieties, forms a stable activator-sensitizer conglomerate via internal conversion (IC) and intersystem crossing (ISC), relaxing the excited ligand (sensitizer) and transferring its energy to the central lanthanide ions.[9−11] The constraint in designing such luminescent complexes is the choice of a suitable ligand (i.e., triplet level energies exceeding those of the PL levels of lanthanide ions). In addition, for an effective ligand-to-lanthanide ion energy transfer, a substantial overlap between emission spectrum of the ligand and absorption spectrum of the lanthanide ion is required.[12]

Among various lanthanide complexes, the coordination compound europium(III) β-diketonate is a major research focus[13−15] due to the high PL quantum yield (QY) of Eu^{3+}, as well as the substantial spectral overlap of ligand emission with the Eu^{3+} absorption. Some of these complexes have been employed for temperature sensing and lasing, to name a few applications.[16,17] However, recently, the demand for multifunctional materials has motivated researchers to investigate organic complexes off the common paths in search of a versatile material that is able to address various application tasks.[18] The

Received: December 31, 2014
Accepted: August 4, 2015
Published: August 4, 2015

DOI: 10.1021/acsami.5b06350
ACS Appl. Mater. Interfaces 2015, 7, 18231−18239

β-diketonate, which consists of Eu^{3+}, the ligands 2-theonyltrifluoroacetone (TTA) and 10-phenanthroline (Phen), that is, $Eu(TTA)_3Phen$ (ETP hereafter) demonstrates complementary optical properties serving multiple operations.[19,20]

We present in this work the multifunctionality of this heteropaired complex by revealing various possible photophysical applications such as luminescence-based temperature sensing, laser, UV light detection, and luminescent solar concentrator (LSC) realizations. The material has been prepared as a complex dispersed in poly(vinyl alcohol) (PVA) polymer and ethanol. The TTA ligand strongly absorbs in the UV region and can transfer energy to the central Eu^{3+} ions, and the Phen stabilizes the molecular structure and reduces the nonradiative channels (in absence of Phen, water molecules would remain associated with the complex). Thus, the presence of Phen serves a 2-fold purpose, namely, thermal stability increase and PL enhancement.[10,12]

The ETP itself and its dispersion in PVA effectively absorb UV-A (400−315 nm) and UV−B (315−280 nm) radiations and transfers the energy to the Eu^{3+} ion resulting in PL of considerable intensity. We should stress, that clearly detectable emission is observed as well when the samples are exposed to sunlight (or moderate xenon lamp irradiation). This unique conversion capability of absorption to emission recommends the complex investigated for the realization of UV light detectors and LSCs, while the prototype of the latter is indeed presented herein. Considering the intense and close-to-monochromaticity PL of the Eu^{3+} ion, laser fabrications appear to be in close reach. The hypersensitive nature of the PL intensity of $^5D_0 \rightarrow {}^7F_2$ transition of Eu^{3+} to the ambient conditions opens additional avenues for sensor applications. We demonstrate temperature sensing of the complex covering the range of 50−340 K, allowing applications in cryogenics and biomedicine.

2. EXPERIMENTAL SECTION

2.1. Materials. The following commercial components have been used to produce the samples: europium(III) oxide (99.999%, Alfa Aesar), 2-theonyltrifluoroacetone (99.5%, Otto Kemi), 1,10-phenanthroline (99.5%, Loba Chemie, Pvt. Ltd.), ethanol (Changshu Yangyuan Chemical, China), sodium hydroxide (Qualigens, 99%), PVA (Himedia), hydrochloric acid (Fisher Scientific, 35%), and dichloromethane (Merck, 99.5%).

2.2. Synthesis. Europium chloride was prepared by dissolving europium oxide in diluted hydrochloric acid. To synthesize the ETP, 2-thenoyltrifluoroacetone (6 mmol), 1,10-phenanthroline (2 mmol) and 8 mL of 1N sodium hydroxide were well dissolved in 25 mL of ethanol. In this solution, 2 mmol of $EuCl_3{\cdot}6H_2O$ in 10 mL of distilled water was added dropwise, while constant stirring was maintained. During this process, a white precipitate of the ETP complex was formed. The complex was purified by recrystallization in a mixture of ethanol and dichloromethane. After the purification, the sample was dried under vacuum at 313 K for 24 h. The $Eu(TTA)_3{\cdot}2H_2O$ complex was made by little adaption in the process. To prepare ETP-dispersed PVA films, different complex amounts (0.5, 1, 2.5, 5, 7.5, 10, 15, 20, and 30 wt %) were blended in a fixed amount of PVA using ethanol−water (80/20) mixture as a dispersing medium. Samples were stirred at room temperature until the formation of a clear solution, which was sonicated for 20 min employing the JSP Supersonic Ultrasonic cleaner. Afterward, equal amounts of the solutions were kept in Petri dishes of the same dimension to maintain equal film thicknesses. For the studies, ETP and ETP/PVA film (with ratio of 15/85) were used. For the LSC application, 10 mg of ETP/PVA (2.5/97.5) was incorporated in 2 mL ethanol/water (80/20) and the mixture was sonicated for 20 min, leading to a clear solution. The film investigated was formed on a Corning glass slide by spin coating 30 μL of the solution at 5000 rpm for 50 s using the Laurel spinner model WS-650 MZ-23 NPP. Before starting the experiments, the film was dried at 373 K for 5 h.

2.3. Instrumentation. Fourier transform infrared (FTIR) spectroscopy was performed using the model Spectrum-65 from PerkinElmer in the range of 400−4000 cm^{-1}. The absorption spectrum of the sample was recorded by the Lambda-35 UV−vis spectrophotometer from PerkinElmer. The PL excitation and emission measurements were performed employing the fluorolog-3 spectrofluorometer (FL3−11, Horiba JobinYvon) equipped with a 450 W xenon flash lamp. The lifetime measurements were carried out with a pulsed xenon lamp (25 W) using the same setup. Excitation and emission wavelengths were fixed at 370 and 611 nm, respectively. The nanosecond lifetime monitored at 410 and 432 nm for TTA and Phen was measured by employing a diode laser (model no. EPL-375) emitting at 375 nm with pulse width 73.3 ps. For the UV light sensing experiments, the excitation was provided by a 150 W ozone free xenon lamp (6255, Oriel instruments) whose emission was guided through the 1/4 m Newport Cornerstone monochromator, while the PL intensity was recorded by a fiber monochromator (BLK-C-SR-200, StellarNet, Inc.). Sensor stability and PL temperature dependence were investigated exposing the sample to the 405 nm continuous wave (cw) emission of a diode laser (MDL-III-405, Changchun New Industries Optoelectronics Tech. Co., Ltd.). The PL was monitored using a photomultiplier tube (DPM-HV) attached to a monochromator (Horiba JobinYvon, iHR 320). For the studies at low temperatures, the sample was mounted in an optical cryostat (ARS, Inc., No: DE-202AE) and excited with the MDL-III-405. The PL was recorded using the Ocean Optics QE 65000 fiber monochromator. To be able to measure the PL in the physiological temperature range, we used standard heating equipment (Torsion Spinot DIGITAL Stirrer MC02). The emission in sunlight was measured with a focusing lens and the Ocean Optics QE 65000 as well. The current−voltage ($I-V$) characteristics of the photovoltaic (PV) modules was measured under irradiation of a solar simulator (Oriel Sol3A Class AAA Solar Simulator, 450W, AM1.5, 100 mW/cm^2) and a Keithley 2400 10A sourcemeter (Keithley Instruments, Inc. Cleveland, OH).

3. RESULTS AND DISCUSSION

3.1. PL Emission and Excitation. The FTIR and UV/vis analysis given in the Supporting Information (Figures S1 and S2) confirms the complex formation. Here, we study the role of constituent ion/ligand molecules participating in the PL enhancement process of Eu^{3+} ion. Figure 1 shows PL spectra of Phen, TTA, $EuCl_3{\cdot}6H_2O$, $Eu(TTA)_3{\cdot}2H_2O$ and ETP in ethanol solution at 263 nm excitation. The Phen and TTA molecules, despite of the large PL Stokes shift of ∼50 nm, emit in the blue spectral region. As expected, the emission of Eu^{3+} ion in $EuCl_3{\cdot}6H_2O$ ethanol solution is very weak. In $Eu(TTA)_3{\cdot}2H_2O$ complex, the emission of TTA molecule is quenched, nevertheless, there is a little enhancement in the Eu^{3+} ion PL. We conclude therefore that an energy transfer, although rather weak, from TTA to Eu^{3+} takes place. In contrast, referring to Figure 1b, the ETP shows a significant enhancement in PL of Eu^{3+} ion. Most probably, the Phen molecule significantly reduces the nonradiative channels by replacing water molecules and transfers its energy through singlet and triplet levels (the energy transfer processes are discussed in detail in following sections).

The photophysics of ETP embedded in PVA has been studied, which improves the processability of the complex, making it more applicable for technological usages (thermal and photostability of the complex itself and dispersed in PVA are given in the in Figures S3 and S4 of the Supporting Information). The PL spectra excited at 348 nm of the ETP itself and dispersed in PVA are shown in Figure 2. The PL lines at 579, 589, 611, 652, and 703 nm, correspond to $^5D_0 \rightarrow {}^7F_j$

DOI: 10.1021/acsami.5b06350
ACS Appl. Mater. Interfaces 2015, 7, 18231−18239

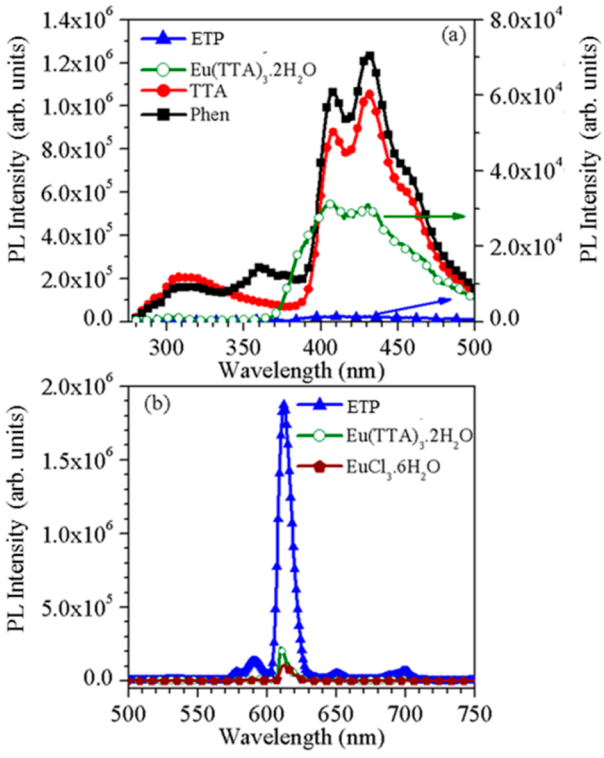

Figure 1. PL spectra of Phen, TTA, $EuCl_3{\cdot}6H_2O$, $Eu(TTA)_3{\cdot}2H_2O$, and the ETP in ethanol solution measured at λ_{ex}= 262 nm for the spectral ranges of (a) UV to green and (b) green to red.

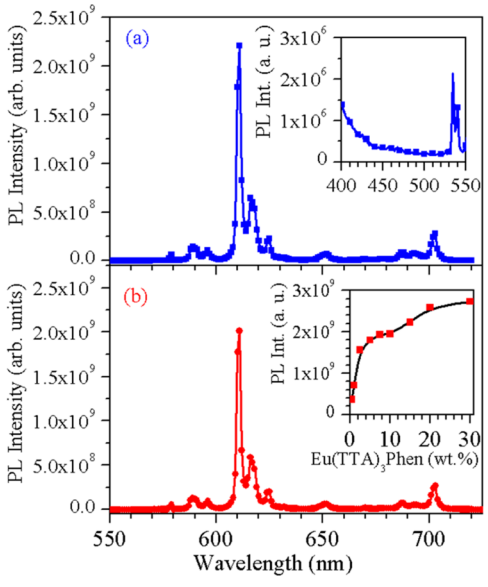

Figure 2. PL spectra of (a) the ETP itself and (b) dispersed in PVA. (a, inset) PL spectrum of the ETP in the range of 400−550 nm and (b, inset) variation in PL intensity at 611 nm in PVA film as a function of the ETP concentration.

transitions (j = 0, 1, 2, 3, and 4, respectively), while the peak at 534 nm originates from the $^5D_1 \rightarrow {}^7F_1$ transition of the Eu^{3+} ion. With the exception of the $^5D_0 \rightarrow {}^7F_1$ transition, which does not depend on the local electric ligand field, is enabled by magnetic dipole mechanisms, all other observed PL peaks are induced by electric dipole transitions. The most intense PL and rather narrow full width at half-maximum (fwhm) (fwhm ∼1.5 nm) peak observed at 611 nm (i.e., the $^5D_0 \rightarrow {}^7F_2$ transition) is

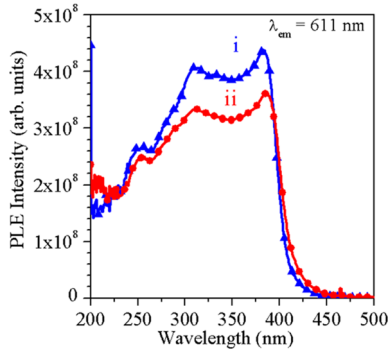

Figure 3. PLE spectra of (i) the ETP and (ii) the ETP dispersed in PVA.

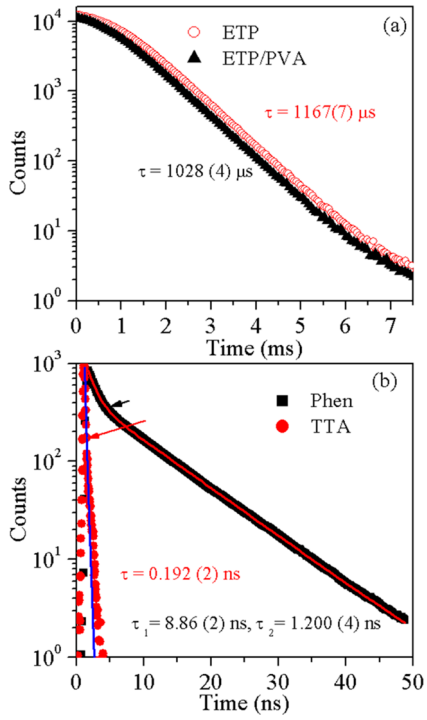

Figure 4. (a) PL decay curves of the ETP itself and dispersed in PVA, recorded by exciting at 370 nm and monitoring the PL at 611 nm. The lifetime was calculated by monoexponential curve fitting. (b) Decay of Phen and TTA recorded by exciting at 375 nm and monitoring the PL at 432 and 410 nm, respectively.

hypersensitive to the local environment and is responsible for the bright, and clearly visible red emission. The more intense $^5D_0 \rightarrow {}^7F_2$ signal in comparison to the $^5D_0 \rightarrow {}^7F_1$ one indicates that the electric ligand field surrounding Eu^{3+} ion is highly polarizable.[12] The intensity ratio (R) of the $^5D_0 \rightarrow {}^7F_2$ to the $^5D_0 \rightarrow {}^7F_1$ transition, also called the monochromaticity, is found to be 15.11 and 16.32 for the plain ETP and the film dispersed in PVA, respectively. The high R value confirms that the samples possess potential to be used in various light emitting applications. The PL intensities of both the samples investigated in Figures 2 are within the same order of magnitude. The inset in Figure 2b display the PL intensity variations at λ_{em} = 611 nm versus complex concentration in the PVA films. The PL intensity of the PVA film keeps increasing up to 30 wt %. Above this concentration, however, the dispersibility is affected and polymer loses its transparency.

DOI: 10.1021/acsami.5b06350
ACS Appl. Mater. Interfaces 2015, 7, 18231−18239

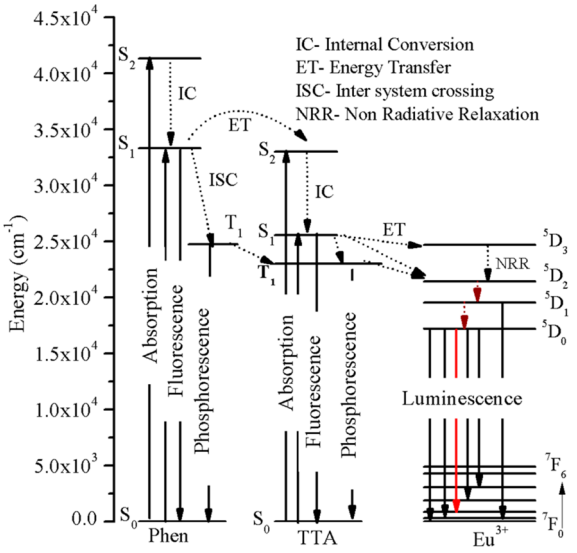

Figure 5. Schematic energy level diagram showing energy transfer process and different transitions in the ETP.

To collect more information about the main emission peak at λ_{em} = 611 of our samples, we measured the PL excitation (PLE) spectra, which are shown in Figure 3. Due to the broad absorption of TTA and Phen, the PLE spectra do not show pronounced structured peaks corresponding to characteristic transitions of the Eu^{3+} ion. This clearly suggests that the PL is basically caused by the energy transfer from the ligand molecules to Eu^{3+} ion. The PLE spectra of the ETP and the ETP/PVA film show peaks at 252, 311, and 383 nm, which are significantly red-shifted with respect to their corresponding absorption peaks (at 228, 263, and 342 nm). Hence, the main energy transfer from the ligands to Eu^{3+}occurs from a lower edge of the absorption bands.

3.2. Lifetime and Energy Transfer Studies. The temporal PL decay of the $^5D_0$ level was monitored at λ_{em} = 611 nm exciting the sample at λ_{ex} = 370 nm. The decay curves of the plain complex and the film dispersed in PVA were fitted using monoexponential function yielding lifetime values of 1167 and 1028 μs, respectively (Figure 4a). We believe that the slight lifetime decrease in the PVA sample is caused by the increase in nonradiative processes.

The energy transfer process from organic ligands to lanthanide ions is also known as "indirect excitation" or "antenna effects".[6] This energy transfer mechanism associates three cascading steps, shown in Figure 5. (1) Spectral overlap of Phen emission spectrum with the absorption spectrum of TTA, subsequently the absorption spectrum overlap of Eu^{3+} ion with the emission spectrum of TTA (Figure S5), that is, presenting a cascading scheme: the optically pumped Phen transfers energy to TTA, whose energy is passed on to Eu^{3+} ion. (2) The first excited state of Phen (S_1) and second excited state of TTA (S_2) are in close proximity, allowing resonance energy transfer (RET) from S_1 to S_2 (or vice versa) under UV excitation at 263 nm. Because the lifetime of Phen (biexponential τ_1 = 8.86 ns, τ_2 = 1.20 ns) is larger than lifetime of TTA (monoexponential τ = 0.19 ns, see Figure 4b), the energy flows from Phen (S_1) to TTA (S_2), and after nonradiative relaxation to S_1 of TTA, the energy will be transferred to the $^5D_3$ level of Eu^{3+} ion. (3) Part of the energy of the Phen S_1 excited state is transferred to the ligand triplet state through ISC. The energy transfer from the triplet state occurs to the resonantly excited level $^5D_2$ of the Eu^{3+} ion. This relaxation path produces PL by 4f−4f transitions.

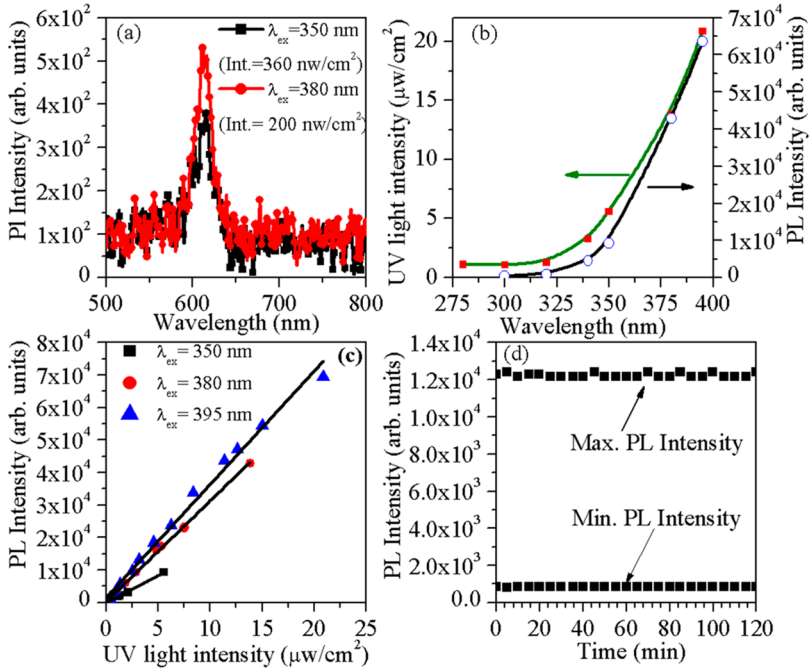

Figure 6. (a) PL spectra of the ETP at different excitation wavelengths and UV light intensities demonstrating the miniscule UV light intensities detected with this sensor. (b) UV light intensity of xenon lamp and corresponding PL signal at different wavelengths (275−400 nm). (c) PL intensity vs UV light intensity of xenon lamp at different wavelengths. (d) Demonstration of the sensor stability. The excitation, which was provided by a diode laser emitting at 405 nm, was chopped with 2 Hz. To visualize the change in PL intensity over number cycles, we plotted maximum and minimum PL intensity at an interval of 5 min.

DOI: 10.1021/acsami.5b06350
ACS Appl. Mater. Interfaces 2015, 7, 18231−18239

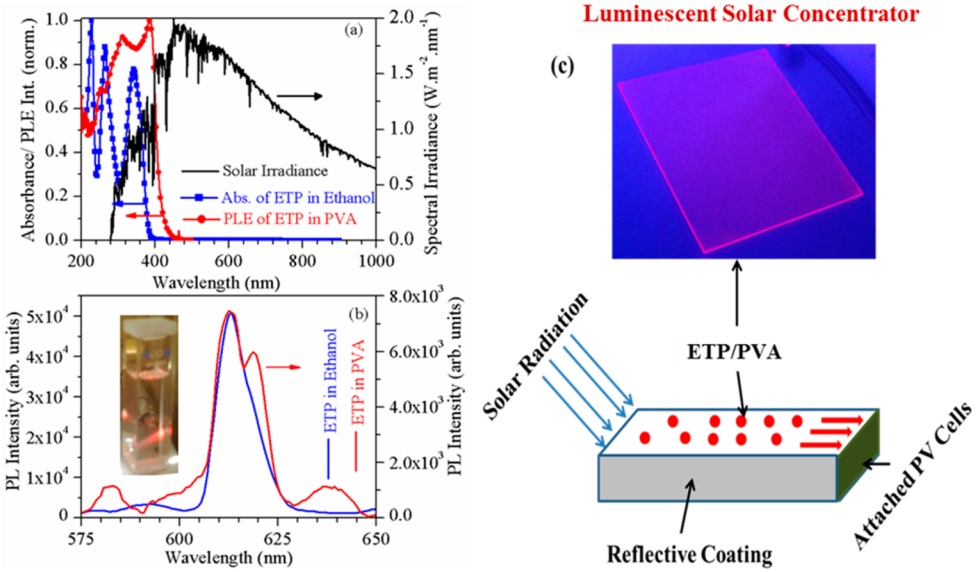

Figure 7. (a) Absorption spectrum of the ETP in ethanol, the PLE spectrum of the ETP dispersed in PVA recorded by monitoring λ_{em} = 611 nm, and the AM1.5 terrestrial solar spectrum. (b) Emission of the ETP dispersed in ethanol and PVA recorded under sunlight excitation and (inset) photo showing red emission under sunlight. (c) Photograph of the ETP/PVA thin film on a glass slide under UV light exposure and a proposed prototype LSC for enhancing the solar cell efficiency.

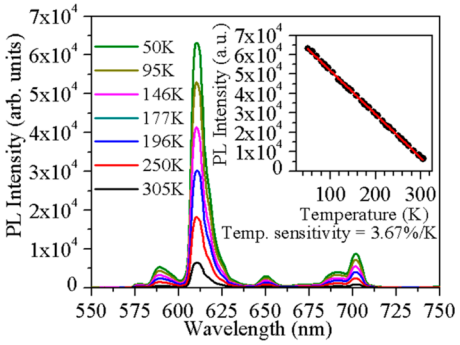

Figure 8. PL spectra of the ETP measured at various temperatures. (Inset) Linear variation of PL intensity at 611 nm as a function of temperature.

We should stress that the difference between the resonance level of the lanthanide ion and the triplet state of the ligand plays a crucial role in the energy transfer process. The maximized energy transfer rate is achieved when the difference between the resonating level is ~2000 cm^{-1}.[6] Exceeding this energy, the overlap between the donor and acceptor spectra will be less, hampering the energy transfer rate. On the other hand, a very small energy difference provokes back energy transfer (thermal deactivation process) from the lanthanide ion to the triplet state of the ligand. The above outlined scenario explains why the energy transfer basically flows from TTA toward the Eu^{3+} ion. Consequently, the ETP complex is capable of producing intense, clearly visible red PL under UV light excitation. This feature promotes the complex for applications as a PL based UV detector and also for LSCs.

3.3. UV Light Detection. While the exposure to UV light at a certain level is known as health hazard, UV radiation finds various applications, such as UV curing and sterilization systems to destroy bacteria in air and water and on medical tools. These mass market applications require efficient and low-cost UV sensing techniques in order to optimize and control the exposure dose. The impinging solar radiations to the earth

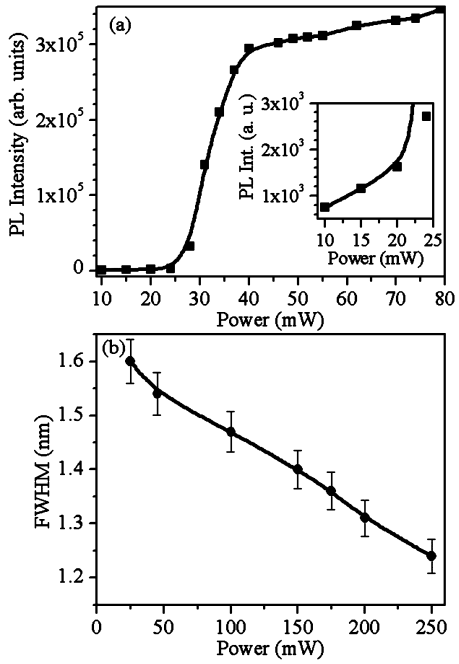

Figure 9. (a) PL intensity and (b) fwhm of the $^5D_0 \rightarrow {}^7F_2$ transition at 611 nm of the ETP dispersed in PVA as a function of impinging light power at 405 nm provided by a cw laser diode.

surface contain the UV-A and UV−B bands. The PLE spectrum in Figure 3 reveals the potential of ETP to convert those radiations into PL, provided it could work with good stability even for very weak radiations.

To our knowledge, lanthanide complexes have not been tested for this specific application. Only a single report by Howie et al.[21] is found reporting the UV sensitivity improvement of cadmium sulfide photoconductors by the use of lanthanide complexes. The objective of the current work is to demonstrate the usefulness of lanthanide complexes for simple, low cost UV sensors with high detectivity. Figure 6a shows the

DOI: 10.1021/acsami.5b06350
ACS Appl. Mater. Interfaces 2015, 7, 18231−18239

Table 1. Observed Lifetime (τ_{obs}), refractive index (n_m) of the Host Material, PL QY (ϕ), Einstein Coefficient (A_E), fwhm of Oscillating Peak ($\Delta\lambda$), and Stimulated Emission Cross Section (σ_s) of the ETP Dispersed in PVA and Its Comparison with the Other Data Reported in Literature

sample	τ_{obs} (μs)	N_m	ϕ	A_E($\times 10^2 s^{-1}$)	$\Delta\lambda$ (nm)	σ_s($\times 10^{-20}$ cm^2)
$Eu(TTA)_3Phen$+ PVA	1028	1.52	0.66	6.43	1.24	4.29
$Eu(hfa)_3(TPPO)_2$[17]	930		0.90		7.0	1.42
$Eu(hfa)_3(OPPO)_2$[17]	1200		0.48		2.1	1.80
$Eu(hfa)_3(BIPHEPO)$[17]	1100		0.87		1.6	4.64

PL spectra of the ETP for the excitations λ_{ex} = 350 nm and λ_{ex} = 380 nm. The experiments have been carried out with a xenon lamp attached to a monochromator (see section 2.3), producing an output intensity of 360 and 200 nW/cm^2, respectively. The clear PL signal indicates that the ETP can detect UV light intensities as low as 200 nW/cm^2. Figure 6b shows the PL intensity variation at λ_{em} = 611 nm as a function of wavelength and intensities of the incident UV light. Figure 6c demonstrates linear growth of the PL intensity with increasing UV light intensities of different wavelengths. We determined the UV sensitivity as a percentage change in PL per μW/cm^2 of UV light and found 117, 108, and 107% per μW/cm^2 for 350, 380, and 395 nm, respectively. The recovery time of the sensor, which is defined by the decay to 10% of the full signal amplitude, is 2.5 ms according to the corresponding decay curve in Figure 4 (a). The sensor's stability was checked by numerous "ON" and "OFF" switching events. To check whether the sample shows optical fatigue, we exposed the ETP to UV laser radiation at 405 nm of 80 mW/cm^2 at 2 Hz frequency for 2 h without detecting an alteration of the material (Figure 6d). The presented results show that lanthanide complexes in general could be very promising for the development of low cost, highly sensitive UV sensors; this property combined with the intense red light PL opens the realistic possibility for LSC realizations, which is discussed in the next section.

3.4. Luminescent Solar Concentrators (LSCs). Currently, the evolving PV technologies for solar energy conversion represent promising avenues for "green", renewable energy generations.[22−24] The real problem to improve the PV efficiency of the conversion of incident photons in electricity lies in the spectral mismatch between the energy distribution of photons in the incident solar spectrum and the band gap of a semiconductor material.[25] In solar cells, particularly in silicon solar cells, the absorption of photons in the range of 250−450 nm (about 15% of terrestrial solar energy) and their conversion into current is very poor. There are many reports on different kinds of materials showing potential to convert this UV radiation in visible emission, but most of them fail under sunlight exposure, which is the essential point of the application discussed here. The ETP in plain form or dispersed in ethanol (or PVA) absorbs the UV-blue part of solar radiation resulting in intense PL at 611 nm, as demonstrated above.

The black curve in Figure 7a shows the AM1.5 terrestrial solar spectrum in the region of interest, namely, the 250−1000 nm region. In addition, the ETP absorption spectrum in ethanol and the PLE spectrum of the ETP in PVA (λ_{em} = 611 nm) are shown by the blue and red curves, respectively. The displayed spectra demonstrate the overlap between solar terrestrial radiation and optical absorption of the hybrid material in the range of 250−450 nm region (where the efficiency of current solar cell is very weak). To demonstrate our concept, we exposed the ETP, which was dissolved in ethanol (10^{-3} M), directly to sunlight. The result was convincing: the samples show strong 611 nm emission without any stark splitting (Figure 7b). The digital photograph of the red emission under sunlight exposure is displayed in the inset.

The photograph in Figure 7c of the ETP/PVA thin film deposited on a glass slide under UV light at 369 nm shows red emission guided to the film edges through internal reflection advocating the film for LSC applications. The emission ratio factor C was determined using the intensity map of the red pixel (in the RGB color model) of the photograhs shown in Figure 7c, and the average intensity ratio between corrected I_{sf} (intensity at the surface) and I_e (intensity at the edges) yields C = 4. The sample's performance as an LSC is given by the collectors's optical conversion efficiency η_{opt}, which is expressed by[26,27]

$$\eta_{opt} = (1 - R)\eta_{abs}\eta_f\eta_s\eta_t\eta_{tr}\eta_{self} \quad (1)$$

representing a measure of the ratio between the output power and the incident optical power, where R is the Fresnel reflection coefficient, $\eta_{abs} = 1 - 10^{-A}$ (A stands for the absorbance at the incident wavelength λ_i) is the ratio of absorbed photons to the number of photons impinging the emitting layer, η_f is the fluorscence quantum yield of the material, η_s is the Stokes efficiency (ratio of the average energy of emitted photons to the average energy of the absorbed ones), $\eta_t = (1 - 1/n_p^2)^{1/2}$, with n_p being the refractive index of the material at the emitted wavelength λ_p, is the trapping efficiency and defined as the fraction of emitted photons that have escaped from the edges versus total emitted photons, η_{tr} is the transport efficiency and takes into account the transport losses due to matrix absorption and scattering, and η_{self} is the self-absorption efficiency arising from self-absorption of the emitters. We calculated $\eta_{opt} \sim 9.5\%$ at 350 nm considering R = 0.0528 (Figure S6), η_{abs} = 0.313 (where A = 0.163 is the absorbance; Figure S6), η_f = 0.749, η_s = 0.572, η_t = 0.749 (n_p = 1.5090, calculated using reflection data, which match well with the refractive index of Corning glass at 612 nm), and $\eta_{tr} = \eta_{self}$ = 1, because the complex thin-film is almost transparent to visible-NIR light and Eu^{3+} ions have negligible self-absorption (no losses). We can certainly improve the optical conversion efficiency of the complex film by increasing its thickness and, consequently, its absorbance. The optical conversion efficiency reported herein exceeds those of Tb^{3+} doped urea bipyrridine bridges organosilanes (1.7%),[28] Eu^{3+} doped urea bipyrridine bridges organosilanes (4.3%),[29] Tb^{3+} based PVA incorporating salicylic acid (8.8%),[27] the cylindrical hollow quantum dot LSC made of PbS incorporated in to PMMA (6.5%),[30] and CdSe/ZnS dispersed in polyurethane and then cast into PMMA molds (2.1%)[31] and is smaller than LSC formed by perylimide incorporated into GLYMO (18.8%).[32] To get experimental evidence for the suitability of the complex material for solar cell, we deposited a thin-film of the ETP/PVA (2.5/97.5) on a PV module with size of 12.5 × 12.5 cm and measured the $I-V$ charateristic of uncoated and

DOI: 10.1021/acsami.5b06350
ACS Appl. Mater. Interfaces 2015, 7, 18231−18239

complex coated PV modules. With the complex, the short circuit current density (J_{sc}) of PV module increases from 37.43 mA/cm^2 to 37.93 mA/cm^2 (Figure S7), pointing toward the capability of the ETP to enhance the PV cell efficiency.

3.5. Temperature Sensing. The PL variations due to temperature changes of the sample reported here open the opportunity to use this material as sensitive temperature sensor. Although, there are several reports for temeperature sensing using lanthanide ions at ambient temperatures, to our knowledge, there are only a few reports on temperature sensing at cryogenic temperature by PL alterations.[33,34] For the demonstration of temperature sensing behavior of the ETP, we have monitored the PL intensity at 611 nm (i.e., the $^5D_0 \rightarrow {}^7F_2$ transition of the Eu^{3+} ion) versus temperature. Figure 8 shows PL spectra of the ETP at various temperatures in the range of 50−305 K, revealing that a temperature decrease remarkably linearly increases the PL intensity. A temperature decrease from 305 to 50 K induces a PL intensity gain of almost 1 order of magnitude because, most likely, of the decrease of nonradiative relaxation channels by damping some of the vibronic modes during cool down. Important for the envisaged application is the fact that the signal changes are fully reversible. The temperature sensitivity can be expressed as % change in PL intensity per K, that is, by the expression $\Delta I/(I_{ref}\Delta T))$, where I_{ref} is the PL intensity at 305 K, ΔT is the change in temperature, and ΔI is the PL intensity variation corresponding to ΔT. The average temperature sensitivity is found to be 3.67% per K, which shows improvement in comparison to the work of Cui et al.[33] (2.299% per K) who used the emission intensity ratio of the $^5D_4 \rightarrow {}^7F_5$ (Tb^{3+}, 545 nm) to $^5D_0 \rightarrow {}^7F_2$ (Eu^{3+}, 613 nm) transition in Eu_xTb_{1-x}DMBDC (DMBDC = 2,5-dimethoxy-1,4-benzenedicarboxylate) complex. Furthermore, the intensity ratio measured in Cui's work shows a linear dependence only in the temeperature range of 50−200 K. In a related work, Brites et al.[34] measured temperature sensing using [Eu(btfa)$_3$(MeOH) (bpeta)] and [Tb(btfa)$_3$(MeOH) (bpeta)] β-diketonate chelates embedded into organic−inorganic hybrid nanoclusters formed by a maghemite (γ-Fe_2O_3) magnetic core coated with a tetraethyl orthosilicate/aminopropyltriethoxysilane (TEOS/APTES) organo-silica shell. The temeperature sensitivity plot shows a Gaussian-like shape, which is less favorable for applications, with a sensitivity maximum of ∼4.9% per K at ∼150 K. Our work, owing to the perfect linear (χ^2 = 0.99) PL intensity variation versus temperature, suggests the employment of the materials for photonic temperature sensing in the temperature range of 50−305 K.

In biological applications, such as hyperthermia, the temperature of targeted organs (e.g., tumors and cancer tissues) are raised locally with respect to the body per se. Hence, to explore in situ possibilities to monitor temperatures in the range of 298−318 K represents an essential research challenge. The suitability of the ETP and its dispersion in PVA to be employed for this task is demonstrated in Figure S8 presenting the linear PL intensity temperature dependence in the range of 305−340 K with sensitivities of 6.5 and 8.6% per K, respectively. Above this temperature, a nonlinear change in PL intensity has been observed, which might be provoked by thermally activated back energy transfers from $^5D_1$ to the ligand's triplet, manipulating the energy transfer efficiency form ligand to Eu^{3+} ions. The investigated ETP dispersed in the biocompatible polymer PVA has the additional advantage of being nontoxic, noninvasive, and capable to operate even in strong electromagnetic fields, and therefore, could find applications in the medical field.

3.6. Toward Laser Realization. Because of the narrow PL with a fwhm of 1.24 nm and intense $^5D_0 \rightarrow {}^7F_2$ transition, the ETP dispersed in PVA is of considerable interest for laser developments. Hasegawa et al.,[17,35,36] have shown amplified spontaneous emission (ASE) in tris(hexafluoroacetylacetonato) europium(III) bis(triphenylphosphine oxide) [Eu(hfa)$_3$(TPPO)$_2$], tris(hexafluoroacetylacetonato) europium(III) 1,2-phenylenebis(diphenylphosphine oxide) [Eu(hfa)$_3$(OPPO)$_2$] and tris(hexafluoroacetylacetonato) europium(III) 1,1′-biphenyl-2,2′-diylbis(diphenylphosphine oxide) [Eu(hfa)$_3$(BIPHEPO)] complexes dispersed in the polyphenylsilsesquioxane (PPSQ) polymer and suggested that these materials could be useful for laser applications. To emphasize this specific application potential of the samples investigated herein, we stress that in Figure 7c, most of the PL is emitted from edges and losses from the glass surface are negligible, which are encouraging features for high-intensity light emitting structures; additionally, we have monitored the PL intensity of ETP dispersed in PVA at 611 nm at different excitation powers provided by a diode laser emitting at 405 nm. The result is displayed in Figure 9a. Up to the excitation of 20 mW the PL intensity increases linearly, while beyond this power an exponential increase in the PL intensity occurs. This sudden exponential increase in PL intensity combined with the PL peak fwhm narrowing shown in Figure 9b are indications for ASE.

Lasing requires a sufficiently large stimulated emission cross-section, which is expressed by[37]

$$\sigma_s(\lambda_s) = \frac{\lambda_s^4}{8\pi c n_m^2 \Delta\lambda} A_E(bJ' : aJ) \tag{2}$$

where, λ_s, c, n_m, $\Delta\lambda$, and A_E are the wavelength (611 nm) of the oscillating peak, the speed of light, the refractive index of the host matrix, fwhm of oscillating peak, and the Einstein coefficient, respectively. The value of A_E can be calculated by using quantum yield (QY) and observed lifetime (τ_{obs}) using the relation $A_E = K_r = QY/\tau_{obs}$, where K_r is the radiative rate. The parameters required to calculate σ_s for the $^5D_0 \rightarrow {}^7F_2$ transition of the PVA sample are listed in Table 1. The value of σ_s is comparable to the one of Nd-Glass lasers ([1.6−4.5] × 10^{-20} cm^2).[37] Additionally, considering the high R-value (∼16.32 in PVA), extremely narrow fwhm (1.23−1.6 nm in PVA), and an ASE factor of ∼2.3, it is expected that the ETP complex dispersed in PVA is a promising candidate for laser applications.

4. CONCLUSION

We have successfully synthesized the ETP and formed hybrids with appealing optical properties by dispersion in PVA. The FTIR studies reveal interaction between Eu and TTA and Phen ligands. The PL studies show order of magnitude enhancements in the PL intensity of Eu^{3+} ion in the presence of TTA and Phen ligands. We have demonstrated the applications of the lanthanide complex for LSC, UV light detection, and temperature sensing and as a prospective laser material. The results demonstrate the multifunctionality of heteropairs formed by the merger of molecules with metal ions.

DOI: 10.1021/acsami.5b06350
ACS Appl. Mater. Interfaces 2015, 7, 18231−18239

■ ASSOCIATED CONTENT

Supporting Information

The Supporting Information is available free of charge on the ACS Publications website at DOI: 10.1021/acsami.5b06350.

FTIR and UV/vis spectra of Phen, TTA, $Eu(TTA)_3 \cdot 2H_2O$, ETP, and their description; thermal and photostability of ETP complex and complex dispersed in PVA; Phen emission and TTA absorption overlap spectrum; TTA emission and Eu^{3+} excitation overelap sepectrum; absorption and reflectance spectra of ETP/PVA (2.5/97.5) deposited on glass slide for LSC application; $I-V$ characteristic of uncoated and ETP/PVA (2.5/97.5) coated crystalline-Si PV module; PL spectra of ETP and ETP dispersed in PVA at different temperatures. (PDF)

■ AUTHOR INFORMATION

Corresponding Author

*E-mail: akhilesh_singh343@yahoo.com.

Author Contributions

The manuscript was written through contributions of all authors. P.K.S. and A.K.S. have contributed equally to this work and both are leading author of this manuscript.

Notes

The authors declare no competing financial interest.

■ ACKNOWLEDGMENTS

P.K.S. acknowledges UGC, India, for the award of the SRF fellowship. A.K.S. and S.K.S. thankfully acknowledge the DGAPA-UNAM program of postdoctoral fellowships and financial support by the Department of Science and Technology (DST), New Delhi, India [INSPIRE Faculty Award No. IFA12-PH-21], respectively. The work was partly supported by the DST project of Prof. S. B. Rai in India and DGAPA-UNAM PAPIIT project TB100213-RR170213 (PI Dr. Bruno Ullrich). We thank Dr. H. Mishra and Dr. P. K. Singh for fruitful discussion and experimental support. The authors acknowledge Robyn M. Duckworth for the criticial reading of the manuscript.

■ REFERENCES

(1) Koppe, M.; Neugebauer, H.; Sariciftci, N. S. Organic Rare Earth Complexes in Polymer Matrices and Light Emitting Diodes. *Mol. Cryst. Liq. Cryst.* **2002**, *385*, 101−111.

(2) Baldo, M. A.; O'Brien, D. F.; You, Y.; Shoustikov, A.; Sibley, S.; Thompson, M. E.; Forrest, S. R. Highly Efficient Phosphorescent Emission from Organic Electroluminescent Devices. *Nature* **1998**, *395*, 151−154.

(3) Wang, F.; Liu, X. Recent Advances in the Chemistry of Lanthanide-Doped Upconversion Nanocrystals. *Chem. Soc. Rev.* **2009**, *38*, 976−989.

(4) Singh, A. K.; Singh, S. K.; Rai, S. B. Role of Li^+ Ion in the Luminescence Enhancement of Lanthanide Ions: Favorable Modifications in Host Matrices. *RSC Adv.* **2014**, *4*, 27039−27061.

(5) Eliseeva, S. V.; Bünzli, J. C. G. Lanthanide Luminescence for Functional Materials and Bio-sciences. *Chem. Soc. Rev.* **2010**, *39*, 189−227.

(6) Yan, B.; Li, Y. Luminescent Ternary Inorganic-Organic Mesoporous Hybrids Eu(TTASi-SBA-15)phen: Covalent Linkage in TTA Directly Functionalized SBA-15. *Dalton Trans.* **2010**, *39*, 1480−1487.

(7) Wang, Z.; Shu, W.; Zhou, Z.; Liu, Y.; Chen, H. Fluorescece Properties and Application of Doping Complexes $Eu_{1-x}L_x(TTA)_3$Phen as Light Conversion Agents. *J. Cent. South Univ. Technol.* **2003**, *10*, 342−346.

(8) Guan, M.; Ma, D.; Liu, S.; Yang, D.; Jiang, J.; Huang, S. $Eu(TTA)_3$phen Nanobelts with Enhanced Luminescent Properties Prepared by Self-assembly. *Chem. Lett.* **2010**, *39*, 886−887.

(9) Bünzli, J.-C. G.; Piguet, C. Taking Advantage of Luminescent Lanthanide Ions. *Chem. Soc. Rev.* **2005**, *34*, 1048−1077.

(10) Singh, A. K.; Singh, S. K.; Prakash, R.; Rai, S. B. Structural and Optical Properties of $Sm(DBM)_3$Phen Doped in Poly(methyl methacrylate) (PMMA): An Evidence for Cascading Energy Transfer Process. *Chem. Phys. Lett.* **2010**, *485*, 309−314.

(11) Luo, Y.; Yan, Q.; Wu, S.; Wu, W.; Zhang, Q. Inter- and Intra-Molecular Energy Transfer During Sensitization of $Eu(DBM)_3$Phen Luminescence by $Tb(DBM)_3$Phen in PMMA. *J. Photochem. Photobiol., A* **2007**, *191*, 91−96.

(12) Singh, A. K.; Singh, S. K.; Mishra, H.; Prakash, R.; Rai, S. B. Structural, Thermal, and Fluorescence Properties of $Eu(DBM)_3Phen_x$ Complex Doped in PMMA. *J. Phys. Chem. B* **2010**, *114*, 13042−13051.

(13) Melby, L. R.; Rose, N. J.; Abramson, E.; Caris, J. C. Synthesis and Fluorescence of Some Trivalent Lanthanide Complexes. *J. Am. Chem. Soc.* **1964**, *86*, 5117−5125.

(14) Binnemans, K. Lanthanide-based Luminescent Hybrid Materials. *Chem. Rev.* **2009**, *109*, 4283−4374.

(15) Sager, W. F.; Filipescu, N.; Serafin, F. A. Substituent Effects on Intramolecular Energy Transfer. I. Absorption and Phosphorescence Spectra of Rare Earth β-Diketone Chelates. *J. Phys. Chem.* **1965**, *69*, 1092−1100.

(16) Peng, H.; Stich, M. I. J.; Yu, J.; Sun, L.-N.; Fischer, L. H.; Wolfbeis, O. S. Luminescent Europium(III) Nanoparticles for Sensing and Imaging of Temperature in the Physiological Range. *Adv. Mater.* **2010**, *22*, 716−719.

(17) Nakamura, K.; Hasegawa, Y.; Kawai, H.; Yasuda, N.; Kanehisa, N.; Kai, Y.; Nagamura, T.; Yanagida, S.; Wada, Y. Enhanced Lasing Properties of Dissymmetric Eu(III) Complex with Bidentate Phosphine Ligands. *J. Phys. Chem. A* **2007**, *111*, 3029−3037.

(18) Singh, S. K.; Singh, A. K.; Rai, S. B. Efficient Dual-mode Multicolor Luminescence in a Lanthanide doped Hybrid Nanostructure: A Multifunctional Material. *Nanotechnology* **2011**, *22*, 275703.

(19) Zhao, S.; Zhang, L.; Li, W.; Li, L. Preparation and Fluorescent Property of $Eu(TTA)_3$Phen Incorporated in Polycarbonate Resin. *Polym. J.* **2006**, *38*, 523−526.

(20) Zhang, R.-J.; Liu, H.-G.; Yang, K.-Z.; Si, Z.-K.; Zhu, G.-Y.; Zhang, H.-W. Fabrication and Fluorescence Characterization of the LB Films of Luminous Rare Earth Complexes $Eu(TTA)_3$Phen and $Sm(TTA)_3$Phen. *Thin Solid Films* **1997**, *295*, 228−233.

(21) Howie, J. A. B.; Rowles, G. K.; Hawkins, P. An Inexpensive Sensor for Ultraviolet-A and Ultraviolet-B Radiation. *Meas. Sci. Technol.* **1991**, *2*, 1070−1073.

(22) Giebink, N. C.; Wiederrecht, G. P.; Wasielewski, M. R. Resonance-Shifting to Circumvent Reabsorption Loss in Luminescent Solar Concentrators. *Nat. Photonics* **2011**, *5*, 694−701.

(23) Sholin, V.; Olson, J. D.; Carter, S. A. Semiconducting Polymers and Quantum Dots in Luminescent Solar Concentrators for Solar Energy Harvesting. *J. Appl. Phys.* **2007**, *101*, 123114.

(24) Singh, A. K.; Singh, S. K.; Kumar, P.; Gupta, B. K.; Prakash, R.; Rai, S. B. Lanthanide Doped Dual-Mode Nanophosphor as a Spectral Converter for Promising Next Generation Solar Cells. *Sci. Adv. Mater.* **2014**, *6*, 405−412.

(25) Huang, X.; Han, S.; Huang, W.; Liu, X. Enhancing Solar Cell Efficiency: The Search for Luminescent Materials as Spectral Converters. *Chem. Soc. Rev.* **2013**, *42*, 173−201.

(26) Correia, S. F. H.; de Zea Bermudez, V.; Ribeiro, S. J. L.; André, P. S.; Ferreira, R. A. S.; Carlos, L. D. Luminescent Solar Concentrators: Challenges for Lanthanide-Based Organic−Inorganic Hybrid Materials. *J. Mater. Chem. A* **2014**, *2*, 5580−5596.

(27) Misra, V.; Mishra, H. Photoinduced Proton Transfer Coupled with Energy Transfer: Mechanism of Sensitized Luminescence of Terbium Ion by Salicylic Acid Doped in Polymer. *J. Chem. Phys.* **2008**, *128*, 244701.

DOI: 10.1021/acsami.5b06350
ACS Appl. Mater. Interfaces 2015, 7, 18231−18239

(28) Graffion, J.; Cojocariu, A. M.; Cattoën, X.; Ferreira, R. A. S.; Fernandes, V. R.; André, P. S.; Carlos, L. D.; Wong Chi Man, M.; Bartlett, J. R. Luminescent Coatings from Bipyridine-Based Bridged Silsesquioxanes Containing Eu^{3+} and Tb^{3+} Salts. *J. Mater. Chem.* **2012**, *22*, 13279−13285.
(29) Graffion, J.; Cattoën, X.; Wong Chi Man, M.; Fernandes, V. R.; André, P. S.; Ferreira, R. A. S.; Carlos, L. D. Modulating the Photoluminescence of Bridged Silsesquioxanes Incorporating Eu^{3+}-Complexed n,n′-Diureido-2,2′-bipyridine Isomers: Application for Luminescent Solar Concentrators. *Chem. Mater.* **2011**, *23*, 4773−4782.
(30) Inman, R. H.; Shcherbatyuk, G. V.; Medvedko, D.; Gopinathan, A.; Ghosh, S. Cylindrical Luminescent Solar Concentrators with Near-Infrared Quantum Dots. *Opt. Express* **2011**, *19*, 24308−24313.
(31) Shcherbatyuk, G. V.; Inman, R. H.; Wang, C.; Winston, R.; Ghosh, S. Viability of Using Near Infrared PbS Quantum Dots as Active Materials in Luminescent Solar Concentrators. *Appl. Phys. Lett.* **2010**, *96*, 191901.
(32) Reisfeld, R.; Shamrakov, D.; Jorgensen, C. Photostable Solar Concentrators Based on Fluorescent Glass Films. *Sol. Energy Mater. Sol. Cells* **1994**, *33*, 417−427.
(33) Cui, Y.; Xu, H.; Yue, Y.; Guo, Z.; Yu, J.; Chen, Z.; Gao, J.; Yang, Y.; Qian, G.; Chen, B. A Luminescent Mixed-Lanthanide Metal−Organic Framework Thermometer. *J. Am. Chem. Soc.* **2012**, *134*, 3979−3982.
(34) Brites, C. D. S.; Lima, P. P.; Silva, N. J. O.; Millán, A.; Amaral, V. S.; Palacio, F.; Carlos, L. D. A Luminescent Molecular Thermometer for Long-Term Absolute Temperature Measurements at the Nanoscale. *Adv. Mater.* **2010**, *22*, 4499−4504.
(35) Hasegawa, Y.; Wada, Y.; Yanagida, S.; Kawai, H.; Yasuda, N.; Nagamura, T. Polymer Thin Films Containing Eu(III) Complex as Lanthanide Lasing Medium. *Appl. Phys. Lett.* **2003**, *83*, 3599.
(36) Nakamura, K.; Hasegawa, Y.; Kawai, H.; Yasuda, N.; Wada, Y.; Yanagida, S. High Lasing Oscillation Efficiency of Eu(III) Complexes having Remarkably Sharp Emission Band. *J. Alloys Compd.* **2006**, *408*−*412*, 771−775.
(37) Snitzer, E. Laser and Glass Technology. *Am. Ceram. Soc. Bull.* **1973**, *52*, 516−525.

DOI: 10.1021/acsami.5b06350
ACS Appl. Mater. Interfaces 2015, 7, 18231−18239